Overconstrained Cable-Driven Parallel Manipulators Statics Analysis Based on Simplified Static Cable Model

Phan Gia Luan and Nguyen Truong Thinh
Department of Mechatronics, Ho Chi Minh City University of Technology and Education, Thu Duc City, Ho Chi Minh City, Vietnam
Email: pgluan95@gmail.com, thinhnt@hcmute.edu.vn

***Abstract*—In recent years, Cable-Driven Parallel Manipulators (CDPM) become more and more interesting topics of robot researchers due to its outstanding advantages. Unlike traditional parallel robots, CDPMs use many flexible cables in order to connect the robot fixed frame and the moving platform instead of using conventional rigid links. Since cables used in CDPM is very light compared to rigid links, its workspace can be very large. Besides, CDPMs are often enhanced load capacity by adding redundant actuators. They also help to widen the singularity-free workspace of CDPM. On the other hand, the redundant actuators produce the underdetermined system i.e. the system has non-unique solutions. Moreover, the elasticity and bendability of flexible cable caused by self-weight and external forces act on it, resulting in the kinematic problem of CDPMs are no longer related to the geometric problem. Therefore, the system of CDPM become non-linear when the deformation of cable is considered. In this study, we introduce the simplified static cable model and use it to linearize the static model of redundantly actuated CDPM. The algorithm to solve the force distribution problem is proposed in section 4. The static-workspace and the performance of those are analyzed in a numerical test.**

***Index Terms*—cable-driven parallel manipulator, CDPM, static analysis, sagging cable, force distribution, workspace**

I. INTRODUCTION

The coupling between the moving platform and robot fixed frame of cable-driven parallel manipulators (CDPM) has fundamental difference from the one of conventional parallel robot. Therefore, approaches used to solve force distribution problem in fixed-links parallel robot are unapplicable in CDPM. Based on recent scientific papers on them, there are many issues that are still leaving behind or not included generally. The main problem of CDPM is caused by the high elasticity and bendability of flexible cable. The force distribution problem becomes more complex since the mass of cable is also taken into account. Erika et al [1] introduced the forward kinematic model for a 4-CDPM. Based on this model, Samir et al [2] proposed collision-free path-planning for the same configuration of CDPM. All of them have practical applications but the positioning accuracy of this kind of model will quickly decrease if CDPM is applied to the larger workspace. Perfectly straightly stress the cable is impossible due to their self-weight and it's easy to see that the length of the cable is closely dependent on the tension force caused by an actuator and load of moving platform. Therefore, the kinematic problem of CDPM doesn't make sense without the presence of static or dynamic problems. Han et al [3] present the effect of sagging cable on the static and dynamic behavior of CDPM and evaluate the pose error of end-effector due to sagging effect in a static state in. They also deal with the effect of cable stretching on system accuracy. Their other study [4] completely established the non-negligible mass cable model in order to provide a full kinematic model of CDPM with the presence of both sagging and elasticity. Merlet and Jean-Pierre [5, 6] determined the solution of the forward kinematic problem by using a heuristic interval analysis approach in a static state. Furthermore, this method also takes care of the overconstrained system where the number of cables of CDPM greater than its degree of freedom. However, it produces large and unbalanced forces distribution that is illustrated in their experiment section.

Another problem that cannot be ignored is redundant actuators in CDPM. In order to increase the load capacity and completely restrain all degrees of freedom of the moving platform [7], many redundant actuators often present in the system, resulting in the overconstrained system. Furthermore, the force distribution problem of redundant resolution CDPM has a non-unique solution. Hence, there was more likely exist set of non-negative tension force and the valid workspace of these kinds of system are larger. However, Tobias et al [8] pointed out that solving these systems are usually expensive in computational time. To the best of our knowledge, numerical approaches are usually applied in order to extract the approximated solution from the undetermined system. Clément et al addressed the force distribution problem in the redundantly actuated system. The unique solution introduced in Ref. [9] is obtained by using a non-iterative algorithm while minimizing the 4-norm of the relative force. Though, this method is not applicable to the

Manuscript received August 11, 2021; revised December 20, 2021.

doi: 10.18178/ijmerr.11.3.159-165

systems that have more than one redundant actuator, in our case is 2. Linear programming employed in Ref. [10] to find safe tension distribution is presented. Hui et al [11] proposed the algorithm to determine the optimal force distribution based on quadratic programming. Andreas [12] introduced the closed-form algorithm based improved force distribution.

In this paper, the simplified static cable model is presented by linearizing the sagging cable model of Irvine [13] in terms of analysis. Thereby, the static problem of CDPM is coordinated with the new cable model to produce a simpler static model that can be solved in real-time. In section 4, an algorithm used to obtain the optimal set of cable tension forces is introduced. The static-workspace is also analyzed in the simulation section with a given certain configuration. The validation of the proposed model is also considered.

II. Static Analysis of Cable Driven Parallel Manipulators and Sagging Cable Model

Our CDPM used in this study is illustrated in Fig. 1. This figure shows the spatial CDPM contained two redundant actuators. This study just takes care of the active segment of cable that traces from bear to the moving platform since the cable segment from an actuator to a pulley is perfectly vertical and its length is almost constant. One more assumption is that the friction on the bears is ignorable. Fig. 2 illustrates the geometric problem of a general CDPM model that is also treated as the kinematic model without the presence of sagging and elasticity. Let {W} be the reference frame located in the robot fixed frame. From now on, any vector without frame denotation is considered in the reference frame. Let {R} = ($\mathbf{P}$(t), $\boldsymbol{\theta}$(t)) be the moving platform frame attached on its body where $\mathbf{P} = [x_P\ y_P\ z_P]^T$ and $\boldsymbol{\theta} = [\alpha_P\ \beta_P\ \gamma_P]^T$ are the position of the center of mass of moving platform and the its orientation respect to {W}. In this study, the ideal static state of CDPM is taken into account which leads to the ith cable of CDPM perfectly lies in the plane that defined by the cable frame {A}. This frame is also illustrated in Fig. 2. Let $\mathbf{A}_i$ and $\mathbf{B}_i$ be the point where ith cable $\mathbf{b}_i^R$ attached to robot fixed frame and moving platform respectively. $\mathbf{b}_i^R$ is the constant vector demonstrates the position where the reaction force of tension $\mathbf{T}_i = [Tx_i\ Ty_i\ Tz_i]^T$ exerts on the end-effector respect to {R}. $\mathbf{b}_i$ can be determined by employing Eq. (1).

$$\mathbf{b}_i = \left({}^W\mathbf{R}_R\right)^T \cdot \mathbf{b}_i^R \tag{1}$$

Where ${}^W\mathbf{R}_R$ is the rotational matrix that presents the transformation from {R} to {W} and can be expressed as Eq. (2). For convenience, C_x and S_x are denoted cos(x) and sin(x) respectively.

$${}^W\mathbf{R}_R = \begin{bmatrix} C\alpha_P C\beta_P & C\alpha_P S\beta_P S\gamma_P - S\alpha_P C\gamma_P & C\alpha_P S\beta_P C\gamma_P + S\alpha_P S\gamma_P \\ S\alpha_P C\beta_P & S\alpha_P S\beta_P S\gamma_P + C\alpha_P C\gamma_P & S\alpha_P S\beta_P C\gamma_P - C\alpha_P S\gamma_P \\ -S\beta_P & C\beta_P S\gamma_P & C\beta_P C\gamma_P \end{bmatrix} \tag{2}$$

Vector $\mathbf{a}_i$ can be treated as the unique solution of inverse kinematic problem of conventional parallel robots. According to Fig. 2, it can be given by Eq. (3).

$$\mathbf{a}_i = \mathbf{P} + \mathbf{b}_i - \mathbf{A}_i = \mathbf{B}_i - \mathbf{A}_i \tag{3}$$

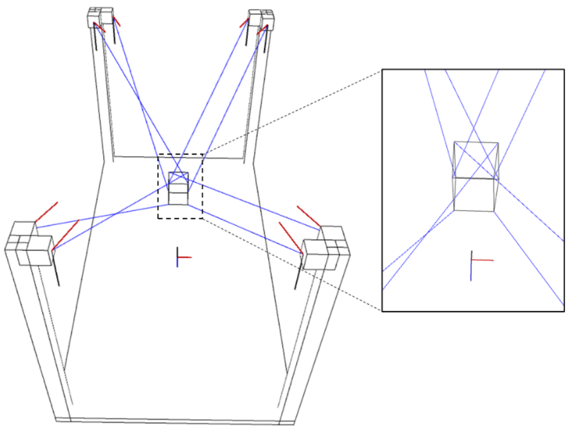

Figure 1. The simulated CDPM with 2 redundant actuators used for checking validation of proposed method.

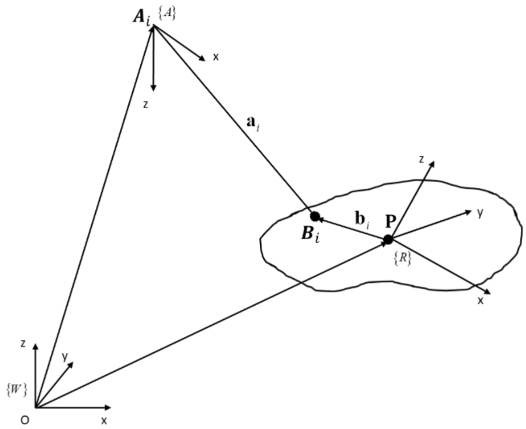

Figure 2. The geometric problem of general CDPM.

However, $\mathbf{a}_i$ cannot be considered as the solution of inverse kinematic problem of CDPM due to the flexible links that are used to connect between robot's fixed frame and moving platform. As discussed, the length of cable just can by exactly determined if static or dynamic problems take part in. Meanwhile, the exact value of length of suspended cable is difficult to extract since its natural complexity. However, the approximated solution of Eq. (3) for CDPM can be determined via the realistic sagging cable model presented by Irvine. This model has been proven usability through several applications such as cable-stayed bridge, improving analysis of CDPM, ship anchor analysis, etc. cable' mass and elongation are also taken into account in Irvine's sagging cable model. Let consider a certain cable illustrated in Fig. 3 has one extremity fixed to $\mathbf{A}$, the other one $\mathbf{B}$ is free and affected by the external force $\mathbf{T^A} = [T^A_x\ T^A_z]^T$. The reaction force at $\mathbf{A}$ is denoted as $\mathbf{T^{A'}}=[T^{A'}_x\ T^{A'}_z]^T$. Let L be the unstrained length of the cable. The ρ, E, A are the linear density, Young's modulus, and ordinary cross-section area of cable respectively. The Cartesian coordinate of $\mathbf{B}$

= $[x_{\mathbf{B}}^A \; z_{\mathbf{B}}^A]^T$ respect to {A} can be given by Eqs. (4) and (5).

$$x_{\mathbf{B}^A} = \frac{T_x^A L}{EA} + \frac{\left|T_x^A\right|}{\rho g}\left[\sinh^{-1}\left(\frac{T_z^A}{T_x^A}\right) - \sinh^{-1}\left(\frac{T_z^A - \rho g L}{T_x^A}\right)\right] \quad (4)$$

$$z_{\mathbf{B}^A} = \frac{T_z^A L}{EA} - \frac{\rho g L^2}{2EA} + \frac{1}{\rho g}\left[\sqrt{\left(T_x^A\right)^2 + \left(T_z^A\right)^2} - \sqrt{\left(T_x^A\right)^2 + \left(T_z^A - \rho g L\right)^2}\right] \quad (5)$$

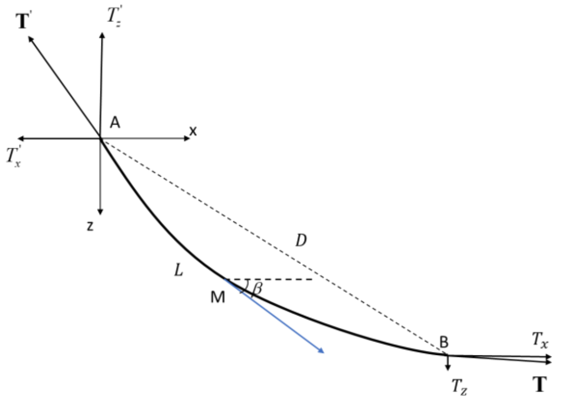

Figure 3. Static equilibrium of a certain cable with the presence of sagging.

It should be noted that the exact solution $\mathbf{T}^A$ cannot be extracted directly from (4) and (5). Let ${}^W\mathbf{R}_{Ai}$ be the rotational matrix that presents transformation from {Ai} to {W} and can be expressed as Eq. (6).

$${}^W\mathbf{R}_{A_i} = \begin{bmatrix} C\theta_i & S\theta_i & 0 \\ 0 & 0 & -1 \end{bmatrix} \quad (6)$$

Where θ_i can be defined by Eq. (7).

$$\theta_i = a\tan 2\left(a_{y_i}, a_{x_i}\right) \quad (7)$$

If only the tensions of cables and load of the moving platform are treated as the external forces exerted on the moving platform then the static equilibrium can be presented by Eqs. (8), (9).

$$\sum_i -T_{x_i}^{A_i}\cos\left(\theta_i\right) = 0 \quad \sum_i -T_{x_i}^{A_i}\sin\left(\theta_i\right) = 0 \quad \sum_i T_{z_i}^{A_i} - mg = 0 \quad (8)$$

$$\sum_i \left(b_{y_i} T_{z_i}^{A_i} + b_{z_i} T_{x_i}^{A_i}\sin\left(\theta_i\right)\right) = 0$$
$$\sum_i \left(-b_{z_i} T_{x_i}^{A_i}\cos\left(\theta_i\right) - b_{x_i} T_{z_i}^{A_i}\right) = 0 \quad (9)$$
$$\sum_i \left(-b_{x_i} T_{x_i}^{A_i}\sin\left(\theta_i\right) + b_{y_i} T_{x_i}^{A_i}\cos\left(\theta_i\right)\right) = 0$$

Since the relationship between length of cable and a force exerts on it, the solution of static problem of general spatial CDPM can be expressed as in Eq. (10).

$$\left[\left\{T_{x_i}^{A_i} \quad T_{z_i}^{A_i}\right\}_{i=1}^{n}\right]^T \quad (10)$$

III. Linearizing the Relationship between T^A_x and T^A_z

According to Irvine's sagging cable model, a unique point BA exists and satisfies the given a certain set of parameters: L, Tx, Tz, ρ, E and A. If the parameter described material of cable, L and Tx is fixed then it can be stated that the Eq. (11) is also the bijective function.

$$f:\left[\mathbf{B}_d^A \quad \varsigma \quad L\right]^T \mapsto \left[T_x^A \quad T_z^A\right]^T \quad (11)$$

Where $\varsigma = [\rho \; E \; A]^T$ is the vector that denotes properties of material that used in cable and $\mathbf{B_d}^A$ is the desired position of the free extremity of considered cable. However, in the inverse kinematic problem of CDPM, *L* is unknown which leads to the problem has non-unique solution. In this section, the relationship between T^A_x and T^A_z with varies *L* will be tried to figure out in order to reduce the number of variables in our system. This relation is proposed by Irvine in [13] but this is just applicable for inextensible cable. However, Dinh Quan et al [14] prove that the cable elastic has a small change in shape of cable as long as $T^A \ll EA$. In this study, the system is assumed that $T^A \ll EA$. Besides, the nonlinear part of the relationship between T^A_x and T^A_z is located where T^A_x belongs to the open interval (0, T_{xmin}). Thereby, this relation can be linearized if the condition $T^A_x \geq T_{xmin}$ was satisfied. Based on these assumptions, the relationship between T^A_x and T^A_z can be given by Eq. (12).

$$T_z^A = a_\pi T_x^A + b_\pi \quad (12)$$

According to Eq. (12), a_π and b_π depend on $[\mathbf{B_d}^A \; \varsigma]^T$. On the other hand, since $T^A \ll EA$, *a* and *b* now only depend on $[\mathbf{B_d}^A \; \rho]^T$.

Let *m* and *α* be the magnitude and heading of tension force $\mathbf{T^A}$ acts on free extremity $\mathbf{B}^A$. *β* is the heading of positioning vector $\mathbf{B_d}^A$ and *D* is its L2-norm respect to {*A*}. The heading of $\mathbf{T^A}$ can be expressed as Eq. (13).

$$\alpha = \tan^{-1}\left(\frac{T_z^A}{T_x^A}\right) \quad (13)$$

According to the relationship between T^A_x and T^A_z given by Eq. (12), the heading of $\mathbf{T^A}$ can be rewritten as Eq. (14).

$$\alpha = \tan^{-1}\left(a_\pi + \frac{b_\pi}{T_x}\right) \quad (14)$$

Let consider the tension force $\mathbf{T^A}$ exert on free extremity $\mathbf{B}^A$ and its reaction force $\mathbf{T^{A'}}$ exerted on the other one. We know that if the cable is perfectly straight then $\mathbf{T^A} + \mathbf{T^{A'}} = 0$. In reality, it's impossible due to weight of the cable itself, resulting in the change of z-axis component of tension along the cable. This explains the phenomenon of not being able to straightly stress the cable. Meanwhile, if T^A_z approach to infinity then weight of the cable can be ignored, resulting in that *α* approaches to *β*. This expression can be given by Eq. (15).

$$\lim_{|T_z|\to\infty} \alpha = \beta \tag{15}$$

Based on the Eq. (12) and Eq. (14), it can be stated that if T^A_z approaches to infinity and a_π is non-zero then α approaches to $\tan^{-1}(a_\pi)$. This express can be given by Eq. (16).

$$\lim_{|T_z|\to\infty} \alpha = \lim_{|T_x|\to\infty}\left(\tan^{-1}\left(a+\frac{b}{T_x}\right)\right) = \tan^{-1}(a) \tag{16}$$

From Eqs. (15) and (16), it can be proved that if Eq. (15) is considered as the relationship between T^A_x and T^A_z then the parameter a_π in the Eq. (12) can be formulated by Eq. (17).

$$a_\pi = \tan(\beta) \tag{17}$$

According to Fig. 3, Let **M** be the point located in cable where the tension force exerts on it is parallel to the chord. In statics, since the resultant force at each point along the cable is affected only by tension cable and gravitational force, the resultant force component along x-axis is not changed over the length of cable. The resultant force component along z-axis is combined between tension cable and its weight, and this component at **M** can be given by Eq. (18).

$$T^A_{z_\mathbf{M}} = \tan(\beta) T^A_x \tag{18}$$

Thereby, the parameter b_π in Eq. (12) depends on the weight of cable segment surrounded by **M** and **B**. It can be stated in Eq. (19).

$$b = \rho g L_{\mathbf{MB}} \tag{19}$$

Where L_{MB} is the length of cable segment **MB**. However, determining exactly L_{MB} is inefficient by its computational time. Furthermore, in CDPM problems, the presence of sagging based on adjusting the cable length not only reduces tension but also reduces cable stiffness if the distance between **M** and chord is large enough. Therefore, the sag of cable should not be large. In fact, the sag depends on **T**. If our assumption $T_x \geq T_{xmin}$ is satisfied and T_{xmin} is large enough, the shape of cable is approximated flat parabola then $L_{MB} \approx D/2$. Thus, the Eq. (12) is completely simplified to Eq. (20).

$$T_z = \tan(\beta) T_x + \frac{\rho g D}{2} \tag{20}$$

IV. Force Distribution on the Overconstrained Cable Driven Parallel Manipulators

The couple of Eqs. (8), (9) present the force distribution of CDPM in a static state. Its solution is easily extracted by applying it for a fully constrained system which usually links the end-effector and robot fixed frame by 6 cables. However, as previous discussion, this problem becomes more complex with the presence of redundant actuators. In this section, we introduced a procedure in order to obtain a feasible set of tension for overconstrained CDPM. By substituting Eq. (20) to Eqs. (8) and (9), the number of variables in the static problem is reduced and these equations can be expressed as Eq. (21).

$$\mathbf{W}\cdot\mathbf{t}_x + \mathbf{b} = \mathbf{0} \tag{21}$$

$$\mathbf{W} = \begin{bmatrix} -\cos(\theta_1) & \dots & -\cos(\theta_n) \\ -\sin(\theta_1) & \dots & -\sin(\theta_n) \\ \tan(\beta_1) & \dots & \tan(\beta_n) \\ b_{y_1}\tan(\beta_1) + b_{z_1}\sin(\theta_1) & \dots & b_{y_n}\tan(\beta_n) + b_{z_n}\sin(\theta_n) \\ -b_{z_1}\cos(\theta_1) - b_{x_1}\tan(\beta_1) & \dots & -b_{z_n}\cos(\theta_n) - b_{x_n}\tan(\beta_n) \\ -b_{x_1}\sin(\theta_1) + b_{y_1}\cos(\theta_1) & \dots & -b_{x_n}\sin(\theta_n) + b_{y_n}\cos(\theta_n) \end{bmatrix} \tag{22}$$

Where **W** presents the wrench matrix given by Eq. (22), $\mathbf{t}_x = [\ T^A_{x1}\ T^A_{x2}\ \dots\ T^A_{xn}]$ is a vector of cable horizontal force components represented in {A}, and **b** is a complement of the static model and it can be obtained by employing Eq. (23).

$$\mathbf{b} = \begin{bmatrix} 0 & 0 & \frac{\rho g}{2}\sum_{i=1}^{n} D_i - mg & \frac{\rho g}{2}\sum_{i=1}^{n} D_i b_{y_i} & -\frac{\rho g}{2}\sum_{i=1}^{n} D_i b_{x_i} & 0 \end{bmatrix}^T \tag{23}$$

The particular solution $\mathbf{t}_x$ of Eq. (21) may determine by finding the pseudo-inverse matrix of **W**, but this may violate the previous assumption $T_{xi} \geq T_{ximin}$ and the worst case is $T_{xi} < 0$. The stiffness matrix is taken into account to tackle this problem in many research [3,4]. However, a disadvantage of this method is high computational time. Therefore, in the very next step, the general solution of Eq. (21) will be determined first and a simple searching technique is employed to determine a feasible particular solution. Firstly, an arbitrary particular solution $\mathbf{t}_{x0} = [\ T^A_{x10}\ T^A_{x20}\ \dots\ T^A_{xn0}]$ is obtained by using the least-squares method. The general solution of Eq. (21) is given by Eq. (24).

$$\mathbf{t}_x = \mathbf{t}_{x_0} + \mathbf{N}\boldsymbol{\lambda} \tag{24}$$

Where **N** is the 6xn matrix that presents the orthonormal basis for the null space of **H** and value of $\mathbf{t}_x$ depends on a vector $\boldsymbol{\lambda} = [\lambda_1\ \lambda_2\ \dots\ \lambda_{n-6}]$. To ensure that cable tensions force is positive, the necessary condition is $T^A_z \geq 0$ that must be satisfied. Thus, there also has condition defined by Eq. (25).

$$T^A_x \geq -\rho g D / 2\tan(\beta) \tag{25}$$

However, it does not guarantee that Eq. (22) is valid. By this reason, the sufficient condition is introduced and given by Eq. (26).

$$\mathbf{t}_x > \mathbf{t}_{x_{\min}}, T_{x_{i\min}} = \frac{-\rho g D_i}{\tan(\beta_i)} + T_{x_i adj} \tag{26}$$

Where $\mathbf{t}_{xmin} = [\ T^A_{x1min}\ T^A_{x2min}\ \dots\ T^A_{xnmin}]$ is the allowable minimum horizontal component cable tension. $T_{xi/adj}$ is the adjusting force to maintain the accuracy of Eq. (22). By employing the Eq. (26) and Eq. (24), the feasible solution set $\boldsymbol{\Theta}_\lambda$ is founded and defined by n-hypercube in $\mathbb{R}^{n-6}$.

To be able to easily illustrate, this procedure is applied to our simulated system illustrated in Fig. 1 with a given certain configuration. Since our system contains 2 redundant actuators, $\mathbf{\Theta}_\lambda$ in this case is a polygon related to $\mathbb{R}^2$ and that is illustrated in Fig. 4. Each line represents the equation (26) with #i represents i[th] cable.

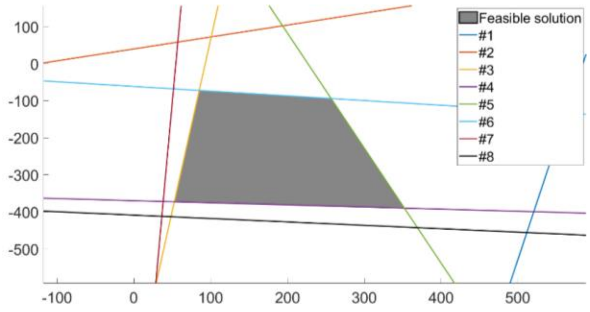

Figure 4. Feasible solution for the certain case of 2-redundant actuators CDPM.

According to Fig. 4, the polygonal boundary of $\mathbf{\Theta}_\lambda$ is determined by the vertex set $\mathbf{\Omega}_\pi = \{\boldsymbol{\lambda}_1, \boldsymbol{\lambda}_2, \ldots, \boldsymbol{\lambda}_h\}$ where h is the number of vertices. In the case illustrated in Fig. 4, $h = 4$. However, a feasible particular solution $\mathbf{t}_x$ cannot directly be determined from $\mathbf{\Theta}_\lambda$ since this set is defined as preimage of feasible tension force set $\mathbf{\Theta}_t$. Thus, $\mathbf{\Theta}_\lambda$ need to be transformed to $\mathbf{\Theta}_t$ via Eq. (24) in order to determine feasible particular solution $\mathbf{t}_x$ later. Since Eq. (24) is an affine transform and $\mathbf{\Theta}_\lambda$ is a hyper-polyhedron in $\mathbb{R}^{n-6}$ then $\mathbf{\Theta}_t$ is also a hyper-polyhedron in $\mathbb{R}^n$. In the example, $\mathbf{\Theta}_\lambda$ is a polygon in $\mathbb{R}^2$ and $\mathbf{\Theta}_t$ is a polygon in $\mathbb{R}^8$. Since the static problem is considered, the feasible particular solution $\mathbf{t}_x$ can take arbitrary in $\mathbf{\Theta}_t$. However, $\mathbf{t}_x$ with minimum L2-norm can be considered as optimum solution of our study. It can be easily obtained by finding the projection of origin on boundary of $\mathbf{\Theta}_t$. According to this procedure, all of feasible particular solution $\mathbf{t}_x$ in the workspace of CDPM can be determined. In the next section, the static-workspace and tension force set in a certain case is considered.

V. Simulation and Results

In order to prove the usability of the proposed method, this method have been applied to our simulated system. This system is a spatial CDPM illustrated in Fig. 1 has two redundant actuators. Thereby, our CDPMs has 8 cables that are used to link 4 poles of robot fixed frame and the moving platform. For convenience, it is also noted that the first cable and the second one is fixed at the bottom right pole according to Fig. 4 and they are numbered clockwise. Their configuration and cable' properties are specified in Table I.

TABLE I. The Configuration of Simulated CDPM.

Workspace	6m x 3m x 3m
End-effector size	0.3m x 0.3m x 0.5m
End-effector load	50 kg
Cable's density	0.09 kg/m
Young's modulus	3.5 GPa
Cross-section area of cable	4 mm2

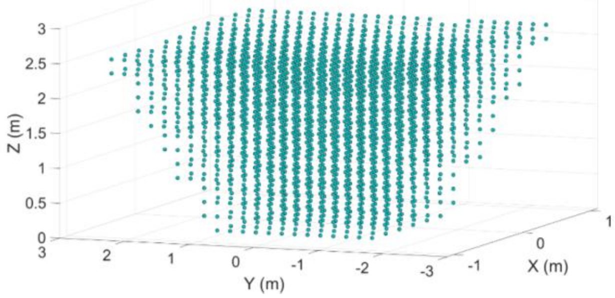

Figure 5. The static-workspace of proposed CDPM with θ = [0 0 0]T.

Firstly, the static-workspace of the mentioned CDPM is established based on the simplified static cable model. Static-workspace is the set of position and orientation of the moving platform in that the static equilibrium Eq. (21) is satisfied. Orientation constraint of {R} is $\boldsymbol{\theta} = [0\ 0\ 0]^T$. Based on numerical simulation, the moving platform is experienced in all workspace of it, the valid positions located inside the polyhedron block defined by out simulated data. This is illustrated in Fig. 5. Since the cable model is simplified and does not fully correct that lead to smaller valid static-workspace. However, it also has a trade-off in computational time, which can perform in real-time. It is also necessary to pay attention to the path planning or obstacle avoidance problem in CDPM, real-time workspace analysis is required. According to the CDPM configuration in table 1 and static-workspace result in Fig. 5, the static-workspace can be defined by a frustum of a rectangular pyramid with Oz as the axis of symmetry. The large base whose size is approximated 1 x 2.4 m^2, while 2.2 x 4.6 m^2 is area of the small base. The distance between two bases is 2.6 m where the small base located at z=0. Based on current constraints, all feasible tension sets in obtained static-workspace are easily constructed by applying Eqs. (24), (26). However, because of high dimensional space, the illustration of them is limited. Thus, the minimum tension force in each feasible tension set is considered and obtaining it by applying full procedure in section 4. After archiving the minimum tension force at this layer by using a numerical approach, these data are continousized and smoothed by employing the non-linear least-square fitting algorithm. Thereby, Fig. 6 indicates the minimum tension force of each cable at each valid position with zP = 1.8 mm in static-workspace. According to the result in Fig. 6, the layer with zP = 1.8 mm has an approximated area of 1.8 x 3.8 m2. In fact, tension force of a particular cable is high when the end-effector approach to the pole where it is fixed to and vice versa. Meanwhile, because of non-symmetric workspace and the limitation of simplified cable model, the maximum of minimum tension forces in the mentioned layer do not approach the pole where it is fixed to, they just approach to near them. Besides, the symmetric in force distribution is still reserved. In order to perform in all of these positions, Txmax should not be smaller than 250N.

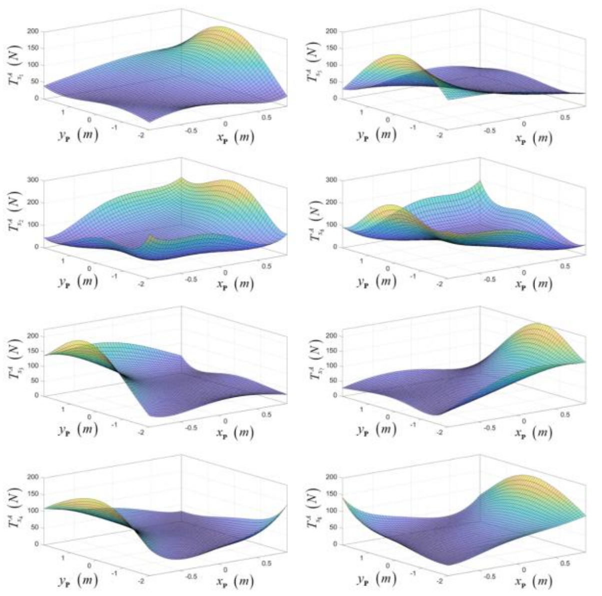

Figure 6. Force distribution along the x-axis respect to {A} in static-workspace with zP = 1.8 mm.

All of simulations have been done on the PC powered by Intel® core™ I3-2100 processor 3.10MHz. The simulation program was written in both Java and MATLAB, and every presented data chart in this paper was plotted in MATLAB. The results show that our proposed method has high-efficiency computational time. By using the code performance measurement of MATLAB, the computational time of method is determined. It takes an average of less than 1ms to find out feasible solution.

VI. Conclusion

In this work, the simplified static cable model was introduced in terms of analysis. Based on that result, the force distribution problem of spatial redundantly actuated CDPM in an ideal static state was established. By fully applying the proposed method in section 4, the minimum set of tension force with a certain configuration is evaluated. The static-workspace is also considered and experimented in a certain case. Our introduced cable model and proposed method to solve the distribution force problem is low computational time and can perform in real-time. However, due to the limitation caused by constraint from Eq. (25), the valid static-workspace is restricted and smaller than in reality. That inspired us for future works:

- Establish the relationship between LMB and Tx instead of approximating LMB ≈ D/2, resulting in the valid static-workspace nearly approach to the real one.
- Quasi-static with low-speed trajectory will be considered and that will produce new challenges in force distribution problems. Besides having to minimize tension force, we also consider to the force distribution over time for continuous and smooth.

Acknowledgment

We thank Ho Chi Minh City University of Technology and Education for supporting this research.

Conflict of Interest

The authors declare no conflict of interest.

Author Contributions

All authors had approved the final version.

References

[1] O. Erika, et al. “A low-cost easy operation 4-cable driven parallel manipulator,” in *Proc. the 2005 IEEE International Conference on Robotics and Automation*, 2005.

[2] L. Samir, et al. “Collision free path-planning for cable-driven parallel robots robotics and autonomous systems,” *Robotics and Autonomous Systems*, vol. 57, no. 11, pp. 1083-1093, 2009.

[3] Y. Han, E. Courteille, et al. “Elastodynamic analysis of cable-driven parallel manipulators considering dynamic stiffness of sagging cables,” in *Proc. 2014 IEEE International Conference on Robotics and Automation (ICRA)*, 2014.

[4] Y. Han, et al. “Vibration analysis of cable-driven parallel robots based on the dynamic stiffness matrix method,” *Journal of Sound and Vibration*, vol. 394, pp. 527-544, 2017.

[5] M. Jean-Pierre and J. Alexandre-dit-Sandretto, “The forward kinematics of cable-driven parallel robots with sagging cables,” *Cable-Driven Parallel Robots*, Springer, Cham, 2015, pp. 3-15.

[6] M. Jean-Pierre, “The kinematics of cable-driven parallel robots with sagging cables: Preliminary results,” in *Proc. 2015 IEEE International Conference on Robotics and Automation (ICRA)*, 2015.

[7] B. Alessandro, Jean-Pierre Merlet et al. “Workspace analysis of redundant cable-suspended parallel robots,” *Cable-Driven Parallel Robots*, Springer, Cham. pp. 41-53, 2015.

[8] B. Tobias, et al. “A new force calculation algorithm for tendon-based parallel manipulators,” in *Proc. 2007 IEEE/ASME International Conference on Advanced Intelligent Mechatronics*, 2007.

[9] Gosselin, Clément, and M. Grenier, "On the determination of the force distribution in overconstrained cable-driven parallel mechanisms," *Meccanica*, vol. 46, no. 1, pp. 3-15, 2011.

[10] Borgstrom, P. Henrik, et al. “Rapid computation of optimally safe tension distributions for parallel cable-driven robots,” *IEEE Transactions on Robotics*, vol. 25, no. 6, pp. 1271-1281, 2009.

[11] L. Hui, et al. “Optimal force distribution based on slack rope model in the incompletely constrained cable-driven parallel mechanism of FAST telescope,” *Cable-driven Parallel Robots*, Springer, Berlin, Heidelberg, 87-102, 2013.

[12] P. Andreas, “An improved force distribution algorithm for over-constrained cable-driven parallel robots,” *Computational Kinematics*, Springer, Dordrecht. 139-146, 2014.

[13] H. M. Irvine, *Cable Structures*, The MIT Press. Cambridge, MA: 15-24, 1981.

[14] Nguyen, D. Quan, et al. “On the simplifications of cable model in static analysis of large-dimension cable-driven parallel robots,” in *Proc. 2013 IEEE/RSJ International Conference on Intelligent Robots and Systems*, 2013.

Phan Gia Luan is graduate student of Ho Chi Minh City University of Technology and Education (Vietnam) with major is mechatronics. He has many years of experience researching in mobile robot, Motion capture, mechatronics, intelligent control. In addition, He also got many scientific research awards.

Nguyen Truong Thinh is Associate Professor of Mechatronics. He obtained his PhD. In 2010 in Mechanical Engineering from Chonnam National University. His work focuses on Robotics and Mechatronic system. Projects include: Service robots, Industrial Robots, Mechatronic system, AI applying to robot and machines, Agriculture smart machines...